Eur. Phys. J. AP **6**, 13–21 (1999)

THE EUROPEAN PHYSICAL JOURNAL APPLIED PHYSICS

Conductivity of a periodic particle composite with spheroidal inclusions*

N. Harfield[a]

Department of Physics, School of Physical Sciences, University of Surrey, Guildford, Surrey GU2 5XH, England

Received: 20 July 1998 / Revised: 13 October 1998 / Accepted: 29 October 1998

Abstract. The effective electrical conductivity of a two-phase material consisting of a lattice of identical spheroidal inclusions in a continuous matrix is determined analytically. The inclusions are located at the node points of a simple-cubic lattice and the axis of rotation of each spheroid coincides with one of the lattice vectors, such that the spheroids are aligned with each other and with the lattice. With an electric field applied in the direction of the rotation axes of the spheroids, the electric potential is found by solving Laplace's equation. The solution is found by analytically continuing the interstitial field into the particle domain and replacing the particles with singular multipole source distributions. This yields an expression for the potential in the interstitial domain as a multipole expansion. Using Green's theorem, it can be shown that only the first coefficient in this expansion is required to determine the effective conductivity of the composite. The coefficients are determined by applying continuity conditions at the particle-matrix boundary and, in a novel approach, this is achieved by transforming the multipole expansion into an expansion in spheroidal harmonics. Results for spheres and prolate and oblate spheroids are compared with experimental data and previous theoretical work, and excellent agreement is observed.

PACS. 41.20.Cv Electrostatics; Poisson and Laplace equations, boundary-value problems – 03.50.-z Classical field theories – 81.05.Qk Reinforced polymers and polymer-based composites

1 Introduction

Calculation of the material properties of a two-phase composite by assuming that the particle phase is arranged according to some kind of lattice structure within a continuous matrix is a classical problem of theoretical physics. The lattice structure imparts periodic behaviour to the solution which allows a large number of particles to be considered. Finite numbers of spherical particles were considered by Maxwell [1] and Rayleigh [2], and since the late 1970s numerous authors have treated an infinite number of particles arranged on various types of cubic lattice. Zuzovsky and Brenner [3] replaced the particles by a singular multipole source distribution located at their centres and determined a solution for a simple-cubic lattice of spheres. McPhedran, McKenzie and Derrick treated simple-cubic [4], body-centred-cubic and face-centred-cubic lattices of spheres [5] by extending Rayleigh's method to include the effects of multipoles of arbitrarily high order. More recently, attempts have been made to generalise the lattice model in a number of ways. Sangani and Yao [6] have attempted to model a less ordered microstructure by placing N spherical particles within a cubic unit cell. This cell is then replicated to form an infinite simple-cubic lattice with a quasi-random distribution of particles. Kushch [7] has treated an orthogonal lattice of aligned spheroids and allowed for some anisotropy in the material of the matrix and the inclusions. Here, the multipole expansion method of Zuzovsky and Brenner is applied to a simple-cubic lattice of aligned spheroidal particles. The spheroidal geometry has the advantage of limiting cases approaching rods or fibres (for large aspect ratio) and discs (as the aspect ratio tends to zero). The novel feature of this solution is the introduction of a transformation matrix which relates the solution in terms of an expansion in higher order multipoles to an expansion in spheroidal harmonics. This allows the continuity conditions at the particle surface to be applied in a straightforward manner to yield an infinite set of linear algebraic equations in the expansion coefficients. It can be shown by use of Green's theorem that only the first coefficient in the expansion is required to calculate the bulk conductivity of the material. This coefficient is determined by solving a truncated equation set.

2 Field equations

There are a number of distinct physical problems which are mathematically equivalent, for example the determination of thermal or electrical conductivity, magnetic permeability or dielectric constant. Here the problem will be discussed in terms of electrical conductivity.

* This paper was presented at the PIERS 98 conference (Progress in Electromagnetics Research Symposium) held at Nantes (France), July 13-17, 1998.

[a] e-mail: n.harfield@surrey.ac.uk

Consider a medium composed of spheroidal particles of conductivity σ_p embedded in a matrix which fills the interstices and has conductivity σ_i. The particles and matrix are assumed to be homogeneous. The aim is to determine $\overline{\overline{\sigma}} = \{\sigma_{ij}\}$, the second-order tensor describing the effective conductivity of the composite. This is done without loss of generality by solving for the electric potential in the medium when an electric field of unit magnitude is applied.

The composite medium is modelled as an infinite lattice of parallelepipedal unit cells, with particles located at lattice points defined by the following set of position vectors:

$$\mathbf{r}_n = n_1\mathbf{a}_1 + n_2\mathbf{a}_2 + n_3\mathbf{a}_3, \quad n_1, n_2, n_3 = 0, 1, 2, \ldots \quad (1)$$

with ($\mathbf{a}_1$, $\mathbf{a}_2$, $\mathbf{a}_3$) a triad of basic lattice vectors characterizing the unit cell. If $\mathbf{J}$ is the local current density vector and Φ is the local electric potential at $\mathbf{r}$, then the basic equations governing steady-state flow are the constitutive relation

$$\mathbf{J}_m(\mathbf{r}) = -\sigma_m \nabla \Phi_m(\mathbf{r}), \qquad \mathbf{r} \in \tau_m, \quad (2)$$

and the zero divergence of the current density

$$\nabla \cdot \mathbf{J}_m(\mathbf{r}) = 0, \qquad \mathbf{r} \in \tau_m, \quad (3)$$

where m = i or p denotes values in the interstitial or particle domains respectively. Equations (2, 3) combine to show that the potential obeys the Laplace equation

$$\nabla^2 \Phi_m(\mathbf{r}) = 0 \quad (4)$$

everywhere. At the surface of a particle, the following condition is derived from the continuity of the tangential electric field:

$$\Phi_\mathrm{i}(\mathbf{r}_{\mathrm{s}+}) = \Phi_\mathrm{p}(\mathbf{r}_{\mathrm{s}-}), \quad (5)$$

where $\mathbf{r}_{\mathrm{s}+}$ and $\mathbf{r}_{\mathrm{s}-}$ denote points on the surface of the particle, approached from the interstitial and particle domains respectively. Continuity of the normal component of current density gives

$$\sigma_\mathrm{i} \frac{\partial \Phi_\mathrm{i}(\mathbf{r}_{\mathrm{s}+})}{\partial n} = \sigma_\mathrm{p} \frac{\partial \Phi_\mathrm{p}(\mathbf{r}_{\mathrm{s}-})}{\partial n}, \quad (6)$$

where n is the coordinate normal to the particle surface.

If a uniform electric field is applied to the material, it gives rise to a potential distribution with average gradient $\langle \mathbf{E} \rangle$. The potential at any point in the composite can be expressed

$$\Phi(\mathbf{r}) = \breve{\Phi}(\mathbf{r}) - \mathbf{r} \cdot \langle \mathbf{E} \rangle, \quad (7)$$

where $\breve{\Phi}(\mathbf{r})$ is a spatially periodic function

$$\breve{\Phi}(\mathbf{r}) = \breve{\Phi}(\mathbf{r} + \mathbf{r_n}). \quad (8)$$

This system of equations possesses a unique solution if either the macroscopic electric field $\langle \mathbf{E} \rangle$ or the macroscopic current density $\langle \mathbf{J} \rangle$ is prescribed. As a consequence of the linearity of this system, there exists a linear macroscopic constitutive relation between the macroscopic current density and electric field:

$$\langle \mathbf{J} \rangle = \overline{\overline{\sigma}} \langle \mathbf{E} \rangle, \quad (9)$$

with $\overline{\overline{\sigma}}$ a second-order conductivity tensor.

3 Multipole expansion solution

3.1 Potential

Equations (2–8) can be solved by analytically continuing the interstitial fields into the interior of the space occupied by the particles and replacing the particles themselves by singular multipole source distributions located at their centres [8]. The sum over all lattice sites is achieved using Fourier analysis, following Hasimoto [9]. This is distinct from the approach of Kushch [7] in which the contribution from each particle is calculated by means of an addition theorem established in the Russian literature. The divergence of the interstitial current is expressed as

$$\nabla \cdot \mathbf{J}_\mathrm{i} = -\sigma_\mathrm{i} \nabla^2 \Phi_\mathrm{i} = -\sum_{j=1}^{\infty} \sum_n \nabla_{(j)} \delta(\mathbf{r} - \mathbf{r}_n) (\cdot)^j \overline{h}_{(j)}, \quad \mathbf{r} \in \tau_\mathrm{i} \oplus \tau_\mathrm{p}, \quad (10)$$

where $\nabla_{(j)}$ is the jth gradient, polyadic operator, $(\cdot)^j$ denotes a j-fold inner product and $\overline{h}_{(j)}$ is a constant tensor of rank j. With some manipulation [3],

$$\overline{h}_{(1)} = \tau_0 \left[\sigma_\mathrm{i} \langle \mathbf{E} \rangle - \langle \mathbf{J} \rangle \right], \quad (11)$$

where $\tau_0 = \mathbf{a}_1 \cdot \mathbf{a}_2 \wedge \mathbf{a}_3$ is the volume of the unit cell. Using (9) and defining $\overline{\overline{\sigma}}^* = \overline{\overline{\sigma}}/\sigma_\mathrm{i}$,

$$\overline{h}_{(1)} = \tau_0 \sigma_\mathrm{i} \left(\overline{\overline{I}} - \overline{\overline{\sigma}}^* \right) \langle \mathbf{E} \rangle, \quad (12)$$

where $\overline{\overline{I}}$ is the *idem* factor. In general, linearity requires that $\overline{h}_{(j)}$ be proportional to $\langle \mathbf{E} \rangle$. Put

$$\overline{h}_{(j)} = \sigma_\mathrm{i} \overline{B}_{(j+1)} \langle \mathbf{E} \rangle \quad (13)$$

with $\overline{B}_{(j+1)}$ a constant tensor of rank $j+1$. This tensor depends only on the geometry of the cubic arrangement, the particle volume fraction and the conductivity ratio $\sigma_\mathrm{p}/\sigma_\mathrm{i} = \alpha$. The general tensorial properties are readily established from crystallographic tables for cubic symmetry. In particular,

$$\overline{B}_{(j+1)} = 0, \qquad \text{for } j \text{ even}. \quad (14)$$

Using equations (7, 10) can be expressed

$$\nabla^2 \breve{\Phi} = \sum_{j=1}^{\infty} \sum_n \nabla_{(2j-1)} \delta(\mathbf{r} - \mathbf{r}_n) (\cdot)^{2j-1} \overline{B}_{(2j)} \langle \mathbf{E} \rangle. \quad (15)$$

Following work by Hasimoto [9], who treated fluid flow past a simple-cubic array of spheres, a solution of (15) can be found using Fourier analysis. The spatial periodicity of $\breve{\Phi}$ permits expansion in the triple Fourier series

$$\breve{\Phi} = \sum_m \phi_m \mathrm{e}^{-2\pi \mathrm{i}\mathbf{k}_m\cdot\mathbf{r}} \tag{16}$$

where

$$\mathbf{k}_m = \frac{1}{\tau_0}\left(m_1\mathbf{b}_1 + m_2\mathbf{b}_2 + m_3\mathbf{b}_3\right), \qquad m_1, m_2, m_3 = 0, \pm1, \pm2, \ldots \tag{17}$$

and $(\mathbf{b}_1, \mathbf{b}_2, \mathbf{b}_3)$ are the basic vectors characterizing the unit cell of the reciprocal lattice. The following is found to be a solution of (15) [3,9]:

$$\breve{\Phi} = \Phi_0 - \frac{1}{4\pi}\sum_{j=1}^{\infty} \nabla_{(2j-1)} S(\cdot)^{2j-1}\, \overline{B}_{(2j)} \langle \mathbf{E}\rangle \tag{18}$$

where Φ_0 is a constant and

$$S = \frac{1}{\pi\tau_0}{\sum_m}' \frac{\mathrm{e}^{-2\pi\mathrm{i}\mathbf{k}_m\cdot\mathbf{r}}}{k_m^2}, \tag{19}$$

with S a solution of

$$\nabla^2 S = 4\pi\left[\frac{1}{\tau_0} - \sum_n \delta\left(\mathbf{r} - \mathbf{r}_n\right)\right]. \tag{20}$$

The sum over m in (19) excludes the value $m = 0$, as indicated by the prime.

The polyadic operator in (10), $\nabla_{(j)}$, regarded as a Cartesian tensor, is completely symmetric in all its indices. No loss of generality arises in regarding $\overline{h}_{(j)}$ as having the same property [3]. In turn, from (13), this same symmetry property may be ascribed to $\overline{B}_{(j)}$. Further, the Cartesian tensor $\overline{B}_{(j)}$ possesses additional symmetry properties based on the fact that its components must remain invariant under group operations appropriate to the symmetry of the cube. It is found that $\overline{B}_{(2)}$ possesses only one independent component and $\overline{B}_{(4)}$ only two, for example. Continuing in this manner it can be established that (18) may be written [3]

$$\breve{\Phi} = \Phi_0 - \frac{1}{4\pi} B \nabla S \langle \mathbf{E}\rangle \tag{21}$$

with B the partial differential operator

$$B = \sum_{m=0}^{\infty}\sum_{n=0}^{\infty}\sum_{p=0}^{\infty} b_{mnp}\frac{\partial^{2(m+n+p)}}{\partial x^{2m}\partial y^{2n}\partial z^{2p}}\,. \tag{22}$$

The b_{mnp} are scalar coefficients to be determined. It is useful to note that S possesses an expansion in spherical harmonics [9]. Expanding about $r = 0$,

$$S = \frac{1}{r} - c + \frac{2\pi r^2}{3\tau_0} + \sum_{n=2}^{\infty}\sum_{m=0}^{m\le n/2} a_{nm} r^{2n} P_{2n}^{4m}(\mu)\cos 4m\phi, \tag{23}$$

in which x, y and z are Cartesian coordinates parallel to the axes of cubic symmetry and $\mu = \cos\theta$ with

$$x = r\sin\theta\cos\phi, \qquad y = r\sin\theta\sin\phi, \qquad z = r\cos\theta. \tag{24}$$

The coefficients c and a_{nm} are listed in Table 13 of [10]:

$$c = 2.8379297, \qquad a_{20} = 3.108227, \qquad a_{30} = 0.5733293. \tag{25}$$

Combining equations (7, 21, 24) gives, for an electric field applied parallel to the z axis,

$$\Phi_{\mathrm{i}} = \Phi_0 - \langle E\rangle\left(\frac{1}{4\pi}B\frac{\partial S}{\partial z} + r\cos\theta\right). \tag{26}$$

3.2 Bulk conductivity

Using equations (13, 12) can be written

$$\overline{B}_{(2)} = \overline{\overline{B}} = \tau_0(\overline{\overline{I}} - \overline{\overline{\sigma}}^*). \tag{27}$$

But $\overline{\overline{B}} = \overline{\overline{I}}B_2$ [3], say, and $b_{000} = B_2$ so

$$b_{000} = \tau_0(1 - \sigma^*) \tag{28}$$

or

$$\sigma^* = 1 - \frac{b_{000}}{\tau_0}\,. \tag{29}$$

Note that, for an array of spheroids or other anisotropic particles, the value of b_{000} (and hence σ^*) will depend on the direction in which the electric field is applied. The above relation can also be determined in an elegant way by application of Green's theorem over the surface of the unit cell [2,4].

4 Harmonic expansion solution

In the spheroidal coordinate system, spheroidal surfaces are surfaces of constant ξ. The polar angle is related to η and ϕ is the azimuthal angle. In general, harmonic solutions of Laplace's equation in a spheroidal system take the form of combinations of Legendre functions of degree n and order m where n and m are integers such that $m = 0, \ldots, n$. For a simple-cubic lattice of spheroids whose axes of rotation (parallel to z) coincide with one of the lattice vectors, the azimuthal symmetry dictates that the order of the Legendre functions must be an integral multiple of 4. If the electric field is also applied parallel to this axis, the potential Φ is odd in the polar variable and consequently the degree of the Legendre functions is also odd. In the case of a prolate spheroid, the potential in the interstitial domain can be written

$$\Phi_{\mathrm{i}} = \Phi_0 + \langle E\rangle\sum_{n=1}^{\infty}\sum_{m=0}^{m<n/2} c_{nm}[P_{2n-1}^{4m}(\xi)P_{2n-1}^{4m}(\eta) + \mathcal{L}_{2n-1}^{4m}Q_{2n-1}^{4m}(\xi)P_{2n-1}^{4m}(\eta)]\cos 4m\phi \tag{30}$$

where

$$\mathcal{L}_s^t = \frac{1-\alpha}{\alpha\left[\dfrac{Q_s^t(\xi_0)}{P_s^t(\xi_0)}\right] - \left[\dfrac{Q_s^t(\xi_0)'}{P_s^t(\xi_0)'}\right]}. \tag{31}$$

In the above, the P_s^t and Q_s^t are Legendre functions of the first and second kinds, respectively. The c_{nm} are unknown coefficients. The coefficients $\mathcal{L}_s^t$ have been determined by using the interface conditions (5, 6) and eliminating coefficients in the expansion for Φ_p in spheroidal harmonics. The expansion for Φ_p contains only growing harmonics, which are of the form $P_{2n-1}^{4m}(\xi)P_{2n-1}^{4m}(\eta)$, since the potential in the particle interior is finite at its centre. The coordinate ξ_0 denotes the surface of the particle and the prime indicates the derivative normal to the surface, *i.e.*

$$Q_s^t(\xi_0)' \equiv \left.\frac{\mathrm{d}Q_s^t(\xi)}{\mathrm{d}\xi}\right|_{\xi=\xi_0}.$$

The solution for oblate spheroids can be obtained directly from that for prolate spheroids by formally replacing ξ with $\mathrm{i}\xi$ and d with $-\mathrm{i}d$, where $2d$ is the distance between the foci of the elliptic cross-section.

In order to solve for the coefficients b_{mnp} defined in (22) and hence determine the bulk conductivity, equation (29), it is necessary to write (26) in terms of spheroidal harmonics. The growing and decaying terms can then be matched with those in (30) and the c_{nm} eliminated to give a set of linear equations which can be solved for the b_{mnp}. Equation (26) can be written in terms of spherical harmonics by using the expansion of S given in (23) and recognising that Cartesian derivatives of spherical harmonics themselves give rise to spherical harmonics. Once the expansion in terms of spherical harmonics has been obtained, it is a simple matter to obtain a solution for spherical particles, but for spheroidal particles a further operation is required. The spherical harmonics must be transformed into spheroidal harmonics. This is achieved by means of the transformation relationships derived in the Appendix.

It is useful to note that the form of B given in (22) is not the most convenient form since operating on each term in S gives rise to a sum of several harmonics. This generates tedious algebra with the potential for errors, as pointed out by Sangani and Acrivos [11] who exploited certain properties of the spherical harmonics to replace the third-order tensor with elements b_{mnp} by a second-order tensor. In the process, an algebraic error in Zuzovsky and Brenner's work [3] was exposed.

As shown in detail in the Appendix, the following transformation relationships have been established for systems of coordinates in which the polar axes of the spherical and spheroidal systems coincide. For the growing harmonics, if s and t are both even, or s and t both odd,

$$R^s P_s^t(\mu) = \sum_{j=0}^{(s-t)/2} A_{s,t+2j}^t P_{t+2j}^t(\xi) P_{t+2j}^t(\eta) \tag{32}$$

and, the inverse relationship,

$$P_s^t(\xi)P_s^t(\eta) = \sum_{j=0}^{(s-t)/2} \alpha_{s,t+2j}^t R^{t+2j} P_{t+2j}^t(\mu). \tag{33}$$

The coordinate R is the radial coordinate scaled with the distance between the centre of the spheroid and one of its foci, d, such that $R = r/d$. If s is even and t is odd, or s odd and t even,

$$R^s P_s^t(\mu) = \sum_{j=0}^{(s-t-1)/2} A_{s,t+1+2j}^t P_{t+1+2j}^t(\xi) P_{t+1+2j}^t(\eta), \tag{34}$$

with

$$P_s^t(\xi)P_s^t(\eta) = \sum_{j=0}^{(s-t-1)/2} \alpha_{s,t+1+2j}^t R^{t+1+2j} P_{t+1+2j}^t(\mu). \tag{35}$$

For each order, t, the coefficients $\alpha_{s,u}^t$ and $A_{s,u}^t$ form a lower-diagonal checkerboard matrix, which means that the growing spherical harmonics can be represented as a finite series of growing spheroidal harmonics, and *vice versa*. For the decaying harmonics,

$$R^{-(s+1)} P_s^t(\mu) = \sum_{j=0}^{\infty} B_{s,s+2j}^t Q_{s+2j}^t(\xi) P_{s+2j}^t(\eta), \tag{36}$$

with the inverse relationship

$$Q_s^t(\xi)P_s^t(\eta) = \sum_{j=0}^{\infty} \beta_{s,s+2j}^t R^{-(s+1+2j)} P_{s+2j}^t(\mu). \tag{37}$$

In this case, the coefficients $\beta_{s,u}^t$ and $B_{s,u}^t$ form an upper-diagonal checkerboard matrix for each order. The decaying spherical harmonics are thus represented as an infinite series of decaying spheroidal harmonics, and *vice versa*. The relationships given in equations (32–37) permit transformation between Laplacian solutions in spherical and spheroidal coordinate systems, as long as the polar axes of the two systems coincide. The calculation of the elements A, B, α and β is described in the Appendix.

The success of the transformation method will be demonstrated by examination of the chosen example of a simple-cubic lattice of spheroids whose axes are aligned with one of the lattice vectors and with the applied electric field. The method has potential for solving a wider range of problems, for example a lattice of spheroids whose axes are tilted with respect to the lattice vectors. It is simply a question of calculating the appropriate transformation matrix. This method also lends itself to generalising the method of Sangani and Yao [6] by placing a number of spheroidal particles in each unit cell. In this way the microstructure of a real composite can be represented in a more realistic way by creating a quasi-random distribution of particles which may also have distributions of size, shape and orientation.

$$b_{000} = 4\pi d^3 \Big\{ \Gamma_1 (\mathcal{L}_1^0)^{-1} + \frac{4\pi d^3}{3\tau_0} + 4a'_{20}\Gamma_2\lambda^5 + 6a'_{30}\Gamma_3\lambda^7 - \frac{\left[4a'_{20}B^0_{13}(\mathcal{L}^0_3)^{-1}\lambda^5 + 2a'_{30}\Gamma_6 B^0_{13}(\mathcal{L}^0_3)^{-1}\lambda^7 + 16(a'_{20})^2 A^0_{33}\lambda^{10} + 8a'_{20}a'_{30}A^0_{33}\Gamma_7\lambda^{12} + 12(a'_{30})^2 A^0_{53}\Gamma_6\lambda^{14}\right]}{\left[B^0_{33}(\mathcal{L}^0_3)^{-1} + 20a'_{30}A^0_{33}\lambda^7\right]} - (a'_{30})^2\left[36\Gamma_4\mathcal{L}^0_5 + 140\Gamma_5\mathcal{L}^4_5\right]\lambda^{14} + \mathcal{O}(\lambda^{18})\Big\}^{-1}, \tag{38}$$

In this example solution, the first four non-zero terms only in the second term of (26) will be considered, to give a solution for b_{000} accurate to λ^7, where $\lambda = d/l$ with l the side length of the unit cell. This approach parallels that of Zuzovsky and Brenner [3] who obtained a solution accurate to γ^7 with $\gamma = r_0/l$, r_0 being the radius of the spherical particles. Greater accuracy can be obtained by including higher-order terms, as in the calculation of Sangani and Acrivos [11].

Inserting (23) into (26), evaluating the derivative with respect to z and the first few derivatives in B gives the first few terms in the expansion solution for $\Phi_{\rm i}$ in spherical harmonics. See equation (59) in [3]. Transforming this result using relations (32, 34, 36) given above yields a solution containing terms with the following combinations of Legendre functions:

$$P_1P_1,\ P_3P_3,\ P_5P_5,\ P_5^4P_5^4\cos 4\phi,$$
$$Q_1P_1,\ Q_3P_3,\ Q_5P_5, Q_5^4P_5^4\cos 4\phi,$$

where the argument of the first Legendre function in each term is ξ and that of the second is η. Matching terms with those in (30) allows elimination of the c_{nm} and determination of the b_{mnp}. Finally one obtains

see equation (38) above

with $a'_{nm} = l^{2n+1}a_{nm}$ and

$$\begin{aligned}
\Gamma_1 &= B^0_{11}/A^0_{11},\\
\Gamma_2 &= A^0_{31}/A^0_{11},\\
\Gamma_3 &= (A^0_{51}/A^0_{11}) - (B^0_{15}/B^0_{55}),\\
\Gamma_4 &= A^0_{55}/B^0_{55},\\
\Gamma_5 &= A^4_{55}/B^4_{55},\\
\Gamma_6 &= 10(A^0_{31}/A^0_{11}) - 3(B^0_{35}/B^0_{55}),\\
\Gamma_7 &= 3(A^0_{53}/A^0_{33}) + 10(A^0_{31}/A^0_{11}) - 3(B^0_{35}/B^0_{55}).
\end{aligned} \tag{39}$$

To obtain (38) the relation $a_{30}/a_{31} = -360$ has also been used [11].

The bulk conductivity of the material can now be calculated by evaluating (38) and substituting into (29). The result for oblate spheroids is obtained from (38) by replacing ξ with iξ and d with $-$id. The numerical evaluation of (38) is relatively straightforward for prolate and oblate spheroids. For spheres, however, the argument ξ_0 in the Legendre functions and their derivatives in $\mathcal{L}^t_s$, equation (31), becomes large and it is better to use the dedicated expression for b_{000} derived in [3] for a lattice of spheres. This may be written

$$b_{000} = 4\pi r_0^3\Big[\mathcal{L}_1^{-1} + \frac{4\pi r_0^3}{3\tau_0} - \frac{16(a'_{20})^2\gamma^{10}}{(\mathcal{L}_3^{-1} + 20a'_{30}\gamma^7)} - 176\mathcal{L}_5(a'_{30})^2\gamma^{14} + \mathcal{O}(\gamma^{18})\Big]^{-1}, \tag{40}$$

with r_0 the sphere radius, $\gamma = r_0/l$ and

$$\mathcal{L}_s = \frac{1-\alpha}{\alpha + (s+1)/s}\,. \tag{41}$$

In (40), equation (66) of [3] has been corrected as suggested in [11].

5 Predictions and validation

The aspect ratio, ϵ, of a spheroid is defined by

$$\epsilon = a/b, \tag{42}$$

where a and b are the lengths of the semi-major and semi-minor axes, respectively. Therefore $\epsilon > 1$ describes a prolate spheroid, $0 \le \epsilon < 1$ describes an oblate spheroid and $\epsilon = 1$ describes a sphere. In principle, the bulk conductivity of a composite formed of a simple-cubic lattice of spheroids can be calculated from (38) for any value of ϵ. Here results are presented for ϵ with values 0.5 (oblate spheroid), 1.0 (sphere) and 2.0 (prolate spheroid) to facilitate comparisons with former theory and experimental data available in the literature. Results are presented for bulk conductivity as a function of particle volume fraction and as a function of the conductivity ratio of the two phases, α.

The volume fraction is defined as the ratio of the volume occupied by the inclusions to the total volume. For this system in which one spheroidal particle occupies each unit cell, the volume fraction has an analytic expression:

$$f = \frac{4\pi ab^2}{3l^3}\,. \tag{43}$$

The maximum volume fraction is achieved when the particles are sufficiently large to touch one another. For prolate spheroids arranged on a cubic lattice, this occurs for $a = l/2$ and for oblate spheroids when $b = l/2$. From (43), the maximum value of f can be expressed

$$f_{\max} = \begin{cases} (\pi\epsilon)/6, & 0 \le \epsilon < 1, \quad \text{oblate spheroid},\\ \pi/6, & \epsilon = 1, \quad \text{sphere},\\ \pi/(6\epsilon^2), & \epsilon > 1, \quad \text{prolate spheroid}. \end{cases} \tag{44}$$

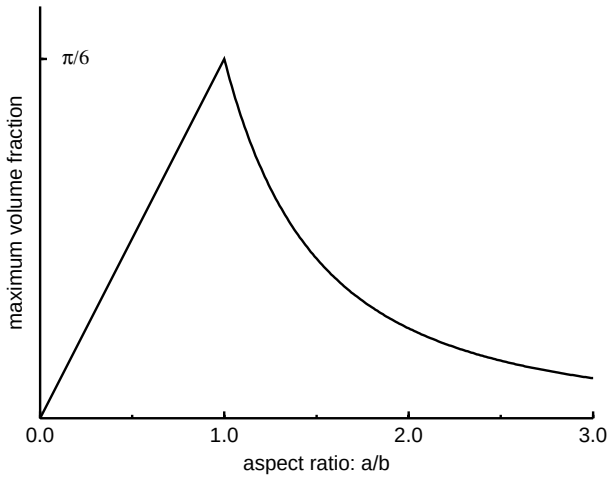

Fig. 1. The maximum particle volume fraction, $f_{\max}$, as a function of particle aspect ratio, ϵ, for a simple-cubic lattice of spheroidal particles with axes of rotation aligned with one of the lattice vectors.

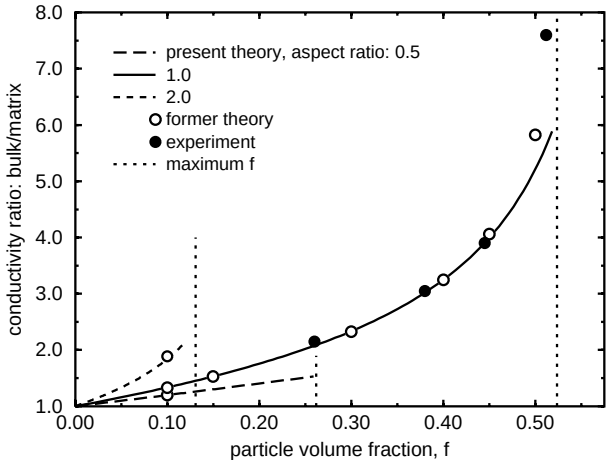

Fig. 2. Bulk conductivity as a function of particle volume fraction for highly conducting particles in an insulating matrix. The results of former theory are taken from [7] and the experimental data is taken from [12].

A graph of $f_{\max}$ *versus* ϵ is plotted in Figure 1. The maximum volume fraction tends to zero as $\epsilon \to 0$, in the limit in which the oblate spheroids become infinitesimally thin discs, and as $\epsilon \to \infty$, when the prolate spheroids become infinitesimally thin rods or fibres.

In Figure 2, predictions of bulk conductivity as a function of volume fraction are compared with experimental data and former theoretical work for highly conducting particles in an insulating matrix ($\alpha \to \infty$). In Figure 3 comparisons are made for insulating particles in a conducting matrix ($\alpha = 0$). The experimental data was obtained from [12]. The experiments were performed using a cubic conductivity cell bounded by lucite walls and silver-plated copper electrodes. Two cells were used. In one, hemispheres of brass and lucite were locked flush against the electrodes to represent high- and low-conductivity particles. The other cell acted as a reference unit and was used to measure the conductivity of the continuous phase (tap water). The conductivity bridge contained symmetrically-shielded components and measurements were taken at bridge frequency high enough to make polarisation errors negligible. In order to measure the conductivity for different values of volume fraction, f, hemispheres of different sizes were used. The independent theoretical results were taken from [7]. As mentioned in Section 2, the calculation in [7] differs from this approach in the way that the infinite number of particles is accounted for. The method adopted here, of representing each particle by a multipole expansion and transforming the solution to deal with spheroidal geometry, lends itself to extension to more general cases in which distributions of particle orientation, size and shape can be considered. In Figures 2 and 3, predictions are shown for values of f approaching $f_{\max}$, *i.e.* up to the limit in which the particles are nearly touching each other. From (44), $f_{\max} = \pi/12$, $\pi/6$ and $\pi/24$ for $\epsilon = 0.5$, 1.0 and 2.0 respectively. There is good agreement between this theory and the experimental data and former theoretical work. The discrepancy between these predictions and other work for conducting particles (Fig. 2) with $\epsilon \geq 1$ as f approaches $f_{\max}$ is due to the fact that in this example only four terms are used in obtaining b_{000} and more are required to accurately describe the field in the interstitial region as the particles approach one another closely. The accuracy could be improved by using a larger number of terms. From Figure 2 it is clear that, for a particular value of f, the bulk conductivity is higher for particles which are elongated in the direction of the applied field, as one would expect. It is also clear from these results that the proposed method of transforming the series solution in spherical harmonics to a solution in spheroidal harmonics using the transformation relationships given in equations (32–37) is successful.

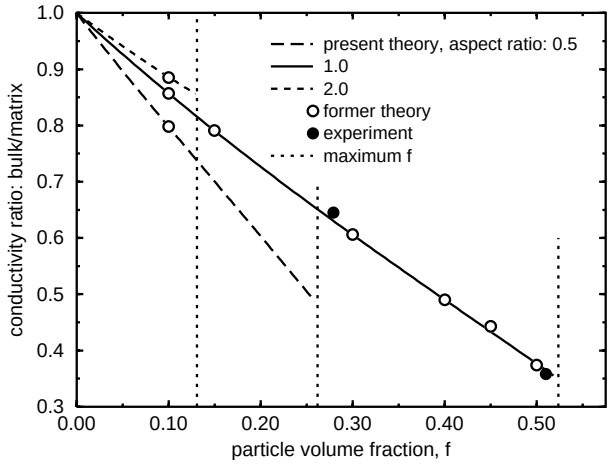

Fig. 3. As for Figure 2 but with insulating particles in a highly conducting matrix.

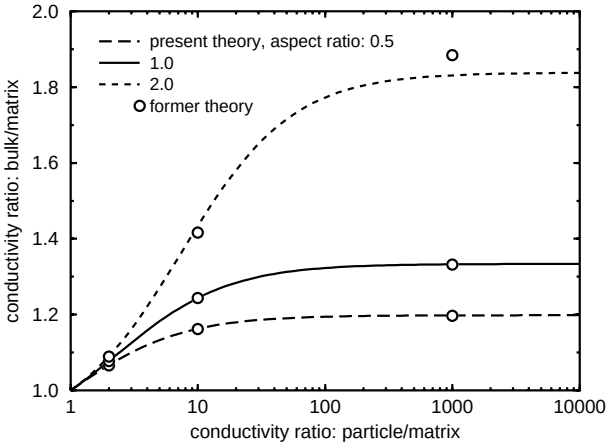

Fig. 4. Bulk conductivity as a function of the particle/matrix conductivity ratio α for $\alpha \geq 1$ and volume fraction 0.1. The results of former theory are taken from [7].

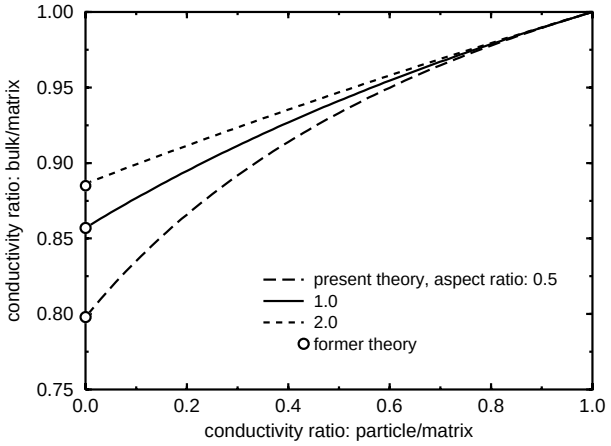

Fig. 5. As for Figure 4 but with $0 \leq \alpha \leq 1$.

In Figures 4 and 5, predictions of bulk conductivity are shown as a function of α for fixed volume fraction $f = 0.1$ and $\epsilon = 0.5$, 1.0 and 2.0. As before, there is excellent agreement between this theory and former theoretical work. The discrepancy observed for prolate spheroids in the high conductivity limit (Fig. 4) is again explained by the low number of terms used in this solution.

6 Conclusion

The bulk conductivity of a two-phase composite consisting of a simple-cubic lattice of spheroidal particles in a matrix with different intrinsic conductivity has been calculated for an electric field applied parallel to the rotation axes of the spheroids, which are aligned with one of the lattice vectors. The novel feature of the solution method is the transformation of a multipole expansion solution for the interstitial field into an expansion in spheroidal harmonics. This facilitates straightforward application of the continuity conditions at the interface between the two phases. Good agreement has been established between theoretical predictions using this method and former theoretical and experimental work [7,12].

The transformation approach coupled with the multipole expansion method lends itself to generalisation in a number of ways. Firstly, spheroids whose axes of rotation are tilted with respect to the lattice vectors and/or the applied field can be treated by computing the appropriate transformation matrix. In addition, following the approach of Sangani and Yao [6], it is possible to place a number of particles in each unit cell to create a less regular microstructure. Allowing more than one particle per unit cell also permits the effect of distributions of particle size, shape (defined by the aspect ratio) and orientation to be modelled. A mixture of particle types can also be considered by allowing the particles to have different values of conductivity. Finally, the effect of a layer on the surface of the particles can be modelled. This would result in a modified form of the coefficient given in (31), and may be useful in considering the case of imperfect contact between the phases.

The author wishes to thank Dr. John R. Bowler for useful discussions and advice. This work was carried out in conjunction with the Polymer Research Centre, School of Physical Sciences, University of Surrey and was supported by an Engineering and Physical Sciences Research Council ROPA.

Appendix: Transformation matrices

The coefficients in the transformation relations (32–37) can be determined in the following manner. Begin by writing

$$P_n^m(\xi)P_n^m(\eta)\cos m\phi = \sum_{s=0}^{\infty}\sum_{t=0}^{s}\alpha_{n,s}^t R^s P_s^t(\mu)\cos t\phi \quad (45)$$

for the growing harmonics and

$$Q_n^m(\xi)P_n^m(\eta)\cos m\phi = \sum_{s=0}^{\infty}\sum_{t=0}^{s}\beta_{n,s}^t R^{-(s+1)} P_s^t(\mu)\cos t\phi \quad (46)$$

for the decaying harmonics, where $\xi = (r_+ + r_-)/2d$, $\eta = (r_+ - r_-)/2d$ with $2d$ the distance between the foci, $r_\pm = (r^2 + d^2 \pm 2dr\mu)^{(1/2)}$ and $\mu = \cos\theta$. The development which follows is given for harmonics which are even in the azimuthal coordinate ϕ. A parallel development applies for harmonics odd in ϕ. Multiplying both sides of (45) by $\cos m\phi$ and integrating over the range of ϕ gives the standard integral [13] (Eqs. (4.3.140, 4.3.141))

$$\int_0^{2\pi}\cos t\phi\cos m\phi\,\mathrm{d}\phi = \begin{cases} 0, & t \neq m, \\ \pi, & t = m, \end{cases} \quad (47)$$

so equation (45) becomes

$$P_n^m(\xi)P_n^m(\eta) = \sum_{s=0}^{\infty}\alpha_{n,s}^m R^s P_s^m(\mu). \quad (48)$$

$$\begin{pmatrix} P_0^0(\xi)P_0^0(\eta) \\ P_1^0(\xi)P_1^0(\eta) \\ P_2^0(\xi)P_2^0(\eta) \\ P_3^0(\xi)P_3^0(\eta) \end{pmatrix} = \begin{pmatrix} 2c_{00} & 0 & 0 & 0 \\ 0 & (2/3)c_{10} & 0 & 0 \\ -c_{00} & 0 & (3/5)c_{20} & 0 \\ 0 & -c_{10} & 0 & (5/7)c_{30} \end{pmatrix} \begin{pmatrix} R^0P_0^0(\mu) \\ R^1P_1^0(\mu) \\ R^2P_2^0(\mu) \\ R^3P_3^0(\mu) \end{pmatrix}, \tag{53}$$

$$\begin{pmatrix} P_1^1(\xi)P_1^1(\eta) \\ P_2^1(\xi)P_2^1(\eta) \\ P_3^1(\xi)P_3^1(\eta) \end{pmatrix} = \begin{pmatrix} (4/3)c_{11} & 0 & 0 \\ 0 & (36/5)c_{21} & 0 \\ -12c_{11} & 0 & (180/7)c_{31} \end{pmatrix} \begin{pmatrix} R^1P_1^1(\mu) \\ R^2P_2^1(\mu) \\ R^3P_3^1(\mu) \end{pmatrix}, \tag{54}$$

$$\begin{pmatrix} P_2^2(\xi)P_2^2(\eta) \\ P_3^2(\xi)P_3^2(\eta) \end{pmatrix} = \begin{pmatrix} (144/5)c_{22} & 0 \\ 0 & (3600/7)c_{32} \end{pmatrix} \begin{pmatrix} R^2P_2^2(\mu) \\ R^3P_3^2(\mu) \end{pmatrix} \tag{55}$$

The orthogonal nature of the Legendre functions is now used to extract the coefficients. Multiplying both sides of (48) by $P_u^m(\mu)$ and integrating over the range of μ gives the standard integral [14] (Eq. (3.12.21))

$$\int_{-1}^{1} P_s^m(\mu)P_u^m(\mu)\mathrm{d}\mu = \begin{cases} 0, & u \neq s, \\ \dfrac{2}{2u+1}\dfrac{(u+m)!}{(u-m)!} = c_{um}^{-1}, & u = s, \end{cases} \tag{49}$$

and (48) becomes

$$\alpha_{n,u}^m R^u = c_{um}\int_{-1}^{1} P_n^m(\xi)P_n^m(\eta)P_u^m(\mu)\mathrm{d}\mu. \tag{50}$$

Following similar steps, (46) becomes

$$\beta_{n,u}^m R^{-(u+1)} = c_{um}\int_{-1}^{1} Q_n^m(\xi)P_n^m(\eta)P_u^m(\mu)\mathrm{d}\mu. \tag{51}$$

Note that $\xi = \xi(r,\mu)$ and $\eta = \eta(r,\mu)$. The combinations $P_n^m(\xi)P_n^m(\eta)$ and $Q_n^m(\xi)P_n^m(\eta)$ give rise to series whose terms each consist of a power of R and a function of μ. For example, for zero order ($m = 0$),

$$P_n^0(\xi)P_n^0(\eta) = R^n f_n(\mu) + R^{n-2}f_{n-2}(\mu) + \ldots + \begin{cases} f_0(\mu), & n \text{ even}, \\ Rf_1(\mu), & n \text{ odd}. \end{cases} \tag{52}$$

Substituting expressions such as (52) into (50) and performing the integration reveals that $P_u^m(\mu)$ acts to pick out from the series the term with the power of R which matches that on the left-hand side of (50), in other words R^u. None of the other terms from (52) contribute. The coefficients $\alpha_{n,u}^m$ have been determined analytically for n, m, u with values 0, 1, 2, 3 with the results

see equations (53, 54, 55) above

and

$$P_3^3(\xi)P_3^3(\eta) = (21600/7)c_{33}R^3P_3^3(\mu). \tag{56}$$

From equations (53–56) it can be seen how expressions (33, 35) arise. In principle, the coefficients can be determined analytically for values of n, m and u greater than 3, but in the absence of an analytic expression for arbitrary values of the indices this is somewhat tedious. In practice the coefficients have been determined by putting $R = 1$ in equations (50, 51) and evaluating the integrals numerically, with the analytical results providing a useful check on the numerical computation. The coefficients A and B in equations (32, 34, 36) are obtained by numerical inversion of the arrays of coefficients α and β.

A further check on the numerical computation is available for the diagonal elements, $n = u$. In this case, the integrals of equations (50, 51) can be evaluated analytically by considering the limit in which $R \to \infty$. In this limit, $\xi \to R$ and $\eta \to \mu$. Taking this limit in equations (50, 51) and integrating with respect to μ using (49) gives

$$\alpha_{n,n}^m R^n = \lim_{R\to\infty} P_n^m(R) \tag{57}$$

and

$$\beta_{n,n}^m R^{-(n+1)} = \lim_{R\to\infty} Q_n^m(R). \tag{58}$$

The values of the Legendre functions $P_n^m(R)$ and $Q_n^m(R)$ in the limit as $R \to \infty$ can be deduced from their hypergeometric series given in reference [13] (Eqs. (8.1.5, 8.1.3)). It is found that

$$\lim_{R\to\infty} P_n^m(R) = \frac{(2R)^n}{\sqrt{\pi}}\frac{\Gamma\left(\frac{1}{2}+n\right)}{\Gamma\left(1+n-m\right)} \tag{59}$$

and

$$\lim_{R\to\infty} Q_n^m(R) = \sqrt{\pi}\,\mathrm{e}^{\mathrm{i}m\pi}(2R)^{-(n+1)}\frac{\Gamma\left(1+n+m\right)}{\Gamma\left(\frac{3}{2}+n\right)}. \tag{60}$$

Putting (59) into (57) and (60) into (58) it is easy to deduce the forms of $\alpha^m_{n,n}$ and $\beta^m_{n,n}$. Using reference [13] (Eqs. (6.1.6, 6.1.8, 6.1.12)), these can be finally written

$$\alpha^m_{n,n} = \frac{1.3.5.7\ldots(2n-1)}{(n-m)!} \tag{61}$$

and

$$\beta^m_{n,n} = \frac{(-1)^m(n+m)!}{1.3.5.7\ldots(2n+1)}\,. \tag{62}$$

References

1. J.C. Maxwell, *A Treatise on Electricity and Magnetism* (Clarendon, Oxford, 1881).
2. R.S. Rayleigh, Phil. Mag. **34**, 481 (1892).
3. M. Zuzovsky, H. Brenner, J. Appl. Math. Phys. **28**, 979 (1977).
4. R.C. McPhedran, D.R. McKenzie, Proc. R. Soc. Lond. A **359**, 45 (1978).
5. D.R. McKenzie, R.C. McPhedran, G.H. Derrick, Proc. R. Soc. Lond. A **362**, 211 (1978).
6. A.S. Sangani, C. Yao, J. Appl. Phys. **63**, 1334 (1988).
7. V.I. Kushch, Proc. R. Soc. Lond. A **453**, 65 (1997).
8. P.M. Morse, H. Feshbach, *Methods of Theoretical Physics* (McGraw-Hill, New York, 1953), Part II, Section 10.3.
9. H. Hasimoto, J. Fluid Mech. **5**, 317 (1959).
10. A.S. Sangani, Ph.D. thesis, Stanford University, 1983.
11. A.S. Sangani, A. Acrivos, Proc. R. Soc. Lond. A **386**, 263 (1983).
12. R.E. Meredith, C.W. Tobias, J. Appl. Phys. **31**, 1270 (1960).
13. M. Abramowitz, I.A. Stegun, *Handbook of Mathematical Functions with Formulas, Graphs and Mathematical Tables*, 9th printing, (Dover, New York, 1972).